Received: 27 October 2025 | Revised: 29 January 2026 | Accepted: 13 February 2026 | Published online: 28 February 2026

RESEARCH ARTICLE

Smart Wearable Technology
2026, Vol. 00(00) 1–9
DOI: 10.47852/bonviewSWT62027989

BON VIEW PUBLISHING

Dual-Model Approach for Knee Osteoarthritis Classification Using Custom CNN and Fine-Tuned VGG16 with Histogram Equalization

G. Prema[1,*], P. Rithanya[1] and A. Shiva Priya[1]

[1] *ECE Department, Mepco Schlenk Engineering College, India*

Abstract: Knee osteoarthritis (KOA) is a progressive joint disorder that often remains asymptomatic in early stages, making timely diagnosis essential. This study presents a deep learning-based framework for KOA classification using preprocessed knee X-ray images. Image enhancement techniques such as histogram equalization and adaptive histogram equalization were applied to improve local contrast. Two independent architectures were developed: a custom convolutional neural network (CNN) designed from scratch and a fine-tuned VGG16 model based on transfer learning. The custom CNN incorporated L1/L2 regularization, batch normalization, and dropout layers to improve generalization. However, initial results revealed reduced performance due to severe class imbalance in the dataset. To address this, data augmentation was employed as an oversampling strategy, using rotation, flipping, translation, shearing, and zoom transformations to balance all KOA grades. To further improve classification performance, an ensemble strategy was introduced by combining the softmax probability outputs of the custom CNN and VGG16 using weighted averaging. This fusion allows the complementary strengths of both models to jointly influence the final Kellgren–Lawrence grade prediction, improving robustness and early-stage KOA detection. Although augmentation increased data diversity, the custom CNN achieved limited accuracy, prompting the adoption of the more robust VGG16 architecture. Comparative evaluation showed that VGG16 and the proposed ensemble achieved superior classification performance, demonstrating the effectiveness of transfer learning for KOA detection. The proposed framework offers a reliable approach for assisting early KOA diagnosis and supporting clinical decision-making.

Keywords: knee osteoarthritis, Kellgren–Lawrence grading, X-ray, classification

1. Introduction

Osteoarthritis (OA) is a degenerative condition characterized by the weakening of cartilage in the knee, resulting in damage or deterioration of the joint. When specifically affecting the knee, it is termed knee osteoarthritis (KOA) [1, 2]. KOA is characterized by the formation of osteophytes (bone growth at the bone edges), sclerosis (tissue hardening), and joint space narrowing (JSN). This study employs a modified CNN [3] to automatically detect and classify KOA. The increasing prevalence of KOA, particularly among the aging population, has made early detection and accurate classification essential for effective management. Traditional diagnostic methods rely heavily on expert radiological assessment using grading systems such as the Kellgren–Lawrence (KL) scale, which can be time-consuming and subjective.

In this study, we present a method for the detection and classification of KOA using convolutional neural networks (CNNs), trained on the Osteoarthritis Initiative (OAI) dataset. Our approach emphasizes achieving high accuracy with a simplified model architecture. While previous works utilized complex ensembles of models such as DenseNet121, DenseNet169, VGG19, and ResNet34 to reach up to 98% accuracy, our custom CNN achieved 75% accuracy. By leveraging the VGG16 model through transfer learning, we significantly improved performance, reaching an accuracy of 96%.

This paper is organized as follows. Section 2 presents the literature review, highlighting relevant studies and existing approaches in the domain. Section 2.1 provides detailed information about the OAI dataset used in this research. Section 3 describes the overall research methodology. Within this section, Section 3.1 explains the preprocessing techniques applied to the dataset. Section 3.2 outlines the proposed custom learning approach based on Convolutional Neural Network (CNN) architecture. Section 3.3 discusses the transfer learning approach using the VGG16 model. Section 3.4 introduces the hybrid ensemble approach that combines multiple models for improved performance. Section 3.5 presents the results and discussion, including performance evaluation metrics such as accuracy, precision, recall, and F1-score. Section 3.6 describes the design and implementation of the user-friendly web interface developed for prediction visualization. Finally, Section 4 concludes the study

***Corresponding author:** G. Prema, ECE Department, Mepco Schlenk Engineering College, India. Email: prema@mepcoeng.ac.in

by summarizing the key findings and suggesting future research directions.

2. Literature Review

Several related studies support this approach. Wang et al. [1] introduced a novel learning scheme that dynamically divides data into two sets—high-confidence and low-confidence samples—based on their reliability. They proposed a hybrid loss function to guide a CNN to learn effectively from both sets. Saini et al. [2] developed semi-automatic and automatic methods for grading KOA severity from plain radiographs. Similarly, Tiulpin and Saarakkala [3] suggested a deep learning (DL) approach relying on model ensembling and transfer learning to build a fully automatic grading pipeline for osteophytes, JSN, and the composite KL grade from knee radiographs. Chen et al. [4] proposed a technique to automatically quantify KOA severity using the KL grading system. Their method utilized a tailored YOLOv2 model for knee joint detection and fine-tuned CNN models with a novel ordinal loss function for KL grade prediction. Nichols et al. [5] explored whether knee acoustic emissions, measured at the point of care using a wearable device, could differentiate knees with pre-radiographic osteoarthritis from normal knees. Badshah et al. [6] conducted biochemical analysis of OA using serum hyaluronic acid enzyme-linked immunosorbent assay and genetic analysis with amplification refractory mutation system Polymerase chain reaction (PCR). Nasser et al. [7] introduced a Discriminative Regularized Auto Encoder to learn discriminative features that enhance classification accuracy. Their experiments on the publicly available OAI dataset demonstrated promising results for early KOA detection. Brahim et al. [8] presented a fully developed computer-aided diagnosis system for early KOA detection based on knee X-rays and machine learning (ML) algorithms.

Zhang et al. [9] proposed a method combining Residual Neural Networks (ResNet) and a convolutional Block Attention Module to detect knee joints in radiographs and automatically predict KL grades. Kim et al. [10] compared the diagnostic performance of DL models with radiologist readings of KL grades and evaluated whether additional patient data could enhance DL performance. Yong et al. [11] recommended treating KL grading as an ordinal classification task rather than a conventional multi-class classification problem.

Antony et al. [12] presented a novel fully CNN to automatically identify knee joints. Aleksei Tiulpin et al. [3] suggested an automated method to estimate KL and Osteoarthritis Research Society International (OARSI) grades using an ensemble of 50-layer residual networks [3].

Mohammed Bany Muhammad et al. (2020) [13] proposed Eigen-CAM, a technique to compute and visualize principal components of learned features from convolutional layers [13]. Rebecca L. Routson et al. [14] demonstrated that a smart cane with vibrotactile feedback helps users with KOA load the cane more effectively, potentially reducing joint stress and slowing disease progression [14].

Hu et al. [15] introduced Adversarial Evolving Neural Network (A-ENN), an adversarial training DL model achieving 62.7% accuracy in predicting KOA progression from baseline X-rays [15]. Jianan Wu et al. [16] linked KOA pain to increased stiffness in certain soft tissues, highlighting the relationship between pain distribution and the nature of tendons and ligaments, which can guide focused therapy [16]. Pierre Dodin et al. [17] proposed a fully automated 3D MRI-based solution to segment and track knee cartilage volume for effective OA monitoring [17]. K. Kubota et al. [18] found that KOA patients exhibit fewer combined muscle synergies and increased co-contraction during walking, presenting potential biomarkers for diagnosis [18].

Xin Chen et al. [19] proposed an entropy-based method using surface Electromyogram (EMG) singnals with fuzzy entropy, achieving 92% accuracy in KOA detection by identifying abnormal muscle co-activation [19]. Manuela Eugster et al. [20] measured knee joint space to inform minimally invasive robotic unicompartmental knee arthroplasty tool design, recommending a 5–8 mm thickness tool for femoral cuts [20].

Zexia He et al. [21] developed a wearable device that reduces knee adduction moment (KAM) by 24.63% in KOA patients and approximates KAM using plantar pressure data and a neural network [21]. Karim and Jiao Jiao et al. [22] presented an explainable approach for KOA diagnosis from radiographs and MRI, achieving 91% accuracy through a deep-stacked transformation pipeline and Region of Interest (ROI) extraction [22]. Soon Bin Kwon et al. [23] and Yong-Woo Lee et al. [24] proposed ML models combining gait analysis and radiographic imaging to classify KOA severity with improved diagnostic accuracy and reliability [23, 24]. Davide Marzorati et al. [25] and Mario Muñoz-Organero et al. [26] introduced DL frameworks using 3D convolutional networks for precise segmentation of the distal femur and proximal tibia from CT scans, critical for customized knee arthroplasty planning [25, 26]. Lior Shamir et al. [27] proposed an automatic approach for OA detection from knee X-rays using a KL-based classifier, achieving high accuracy in grading OA severity to aid clinical decision-making [27].

Tamez-Peña et al. [28] and Chao Wang et al. [29] developed automated methods for knee cartilage and bone segmentation from 3D MRI images with high accuracy and reproducibility in cartilage and bone shape measurements. DL, particularly CNNs, has revolutionized KOA research by enabling automated feature extraction, classification, and segmentation [30–35]. CNN-based models have demonstrated robust performance for KOA diagnosis, severity grading, and progression prediction. Compared to traditional ML, CNNs learn meaningful patterns directly from raw images without handcrafted features, increasing diagnostic efficiency and reducing reliance on expert interpretation.

2.1. Dataset details

In this study, we use a publicly available dataset from the OAI, which contains 9786 knee X-ray images. These images are labeled using the KL grading scale, a widely used system for assessing the severity of KOA. For consistency, all images are resized to 224 × 224 pixels before being input into the model. The KL grading criteria used for classification are summarized in Table 1. The dataset was obtained from Kaggle and can also be accessed through the official OAI website at https://nda.nih.gov/oai. The dataset was split in an 80:20 ratio, with 80% used for training and 20% for testing. Our proposed system aims to accurately classify the severity level of KOA using just a single X-ray image, based on the KL grading system. Sample images representing each grade are shown in Figure 1.

3. Research Methodology

3.1. Preprocessing

To enhance the quality and contrast of knee X-ray images, a series of preprocessing steps was applied. First, resizing was

Table 1
Kellgren and Lawrence grading

Grades	Description	No. of images
Grade 0	Represents the healthy category with no symptoms in the X-ray images	3857
Grade 1	Indicates doubtful category with the presence of joint space narrowing (JSN) and the possibility of osteophytes.	1770
Grade 2	Involves low grade with definite osteophyte formation and potential JSN	2578
Grade 3	Suggests moderate state with more than one osteophyte and potential bone deformity	1286
Grade 4	Represents severe category with large osteophyte formation, definite JSN, and severe sclerosis	295

Figure 1
Sample images of the OAI dataset

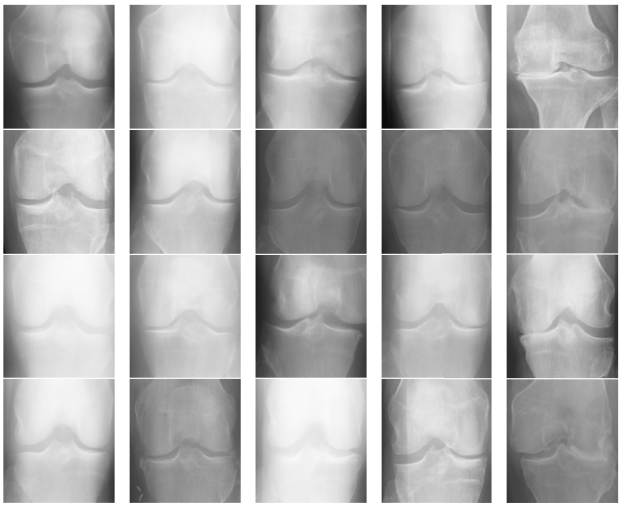

performed to standardize all input images to a resolution of 224 × 224 pixels, aligning with the input requirements of CNN and VGG16 architectures. Second, image enhancement techniques were used, including histogram equalization (HE) and adaptive histogram equalization (AHE). HE is a global contrast enhancement technique that works by redistributing the pixel intensity values across the entire image, thereby producing a more uniform histogram. This technique enhances image contrast using the transformation function:

$$S_k = (L-1)\sum_{j=0}^{k}\frac{n_j}{N} \tag{1}$$

where S_k is the output intensity, L is the total number of gray levels, n_j is the number of pixels with intensity j, and N is the total number of pixels in the image.

While HE improves global contrast, it may cause overbrightness or loss of local detail, as it does not consider spatial variations. To overcome these drawbacks, AHE was applied. AHE enhances local contrast by dividing the image into smaller regions called tiles and applying HE independently within each tile. The resulting intensities are then interpolated to eliminate border artifacts and ensure smooth transitions. The contrast-enhanced intensity $S_{x,y}$ for a pixel (x,y) in AHE is calculated using:

$$S_{x,y} = T_{x,y}(f(x,y)) \tag{2}$$

where $f(x,y)$ is the original intensity of the pixel, $T_{x,y}$ is the local CDF-based transformation function computed from the histogram of the tile containing (x, y), and $S_{x,y}$ is the resulting pixel intensity after local equalization. The enhanced output of HE and AHE is illustrated in Figure 2. The sample preprocessed output of AHE images is illustrated in Figure 3.

Figure 2
Preprocessed images

Figure 3
Sample preprocessed AHE images

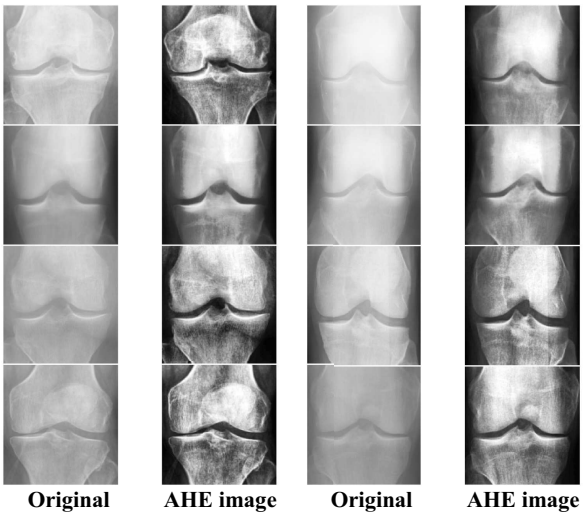

3.2. Custom learning approach: CNN architecture

A custom CNN was designed with increasing filter sizes across layers—Convolutional Layer 1 (C1): 64 filters, Convolutional Layer 2 (C2): 128 filters, Convolutional Layer 3 (C3): 256 filters—and is depicted in Figure 4. Figure 5(a) depicts the 64 activation maps from the first convolutional layer (C1), and Figure 5(b) shows the 128 activation maps from the second convolutional layer (C2). There is a clear increase in feature diversity, with more complex textures and shading patterns emerging. This layer captures mid-level features by combining sets of low-level patterns detected in C1, enabling the identification of curves, blobs, and intersections. Figure 5(c) presents the 256 activation maps from the third convolutional layer (C3). These activations exhibit significant variation in texture complexity and contrast. Some maps show strong activations, while others are subtler, indicating a focus on higher-level abstract patterns. At this stage, the network begins to extract semantic features critical for object recognition and classification tasks. This progression from low-level to high-level feature representation demonstrates the hierarchical learning capability of CNNs.

Figure 4
Custom CNN architecture

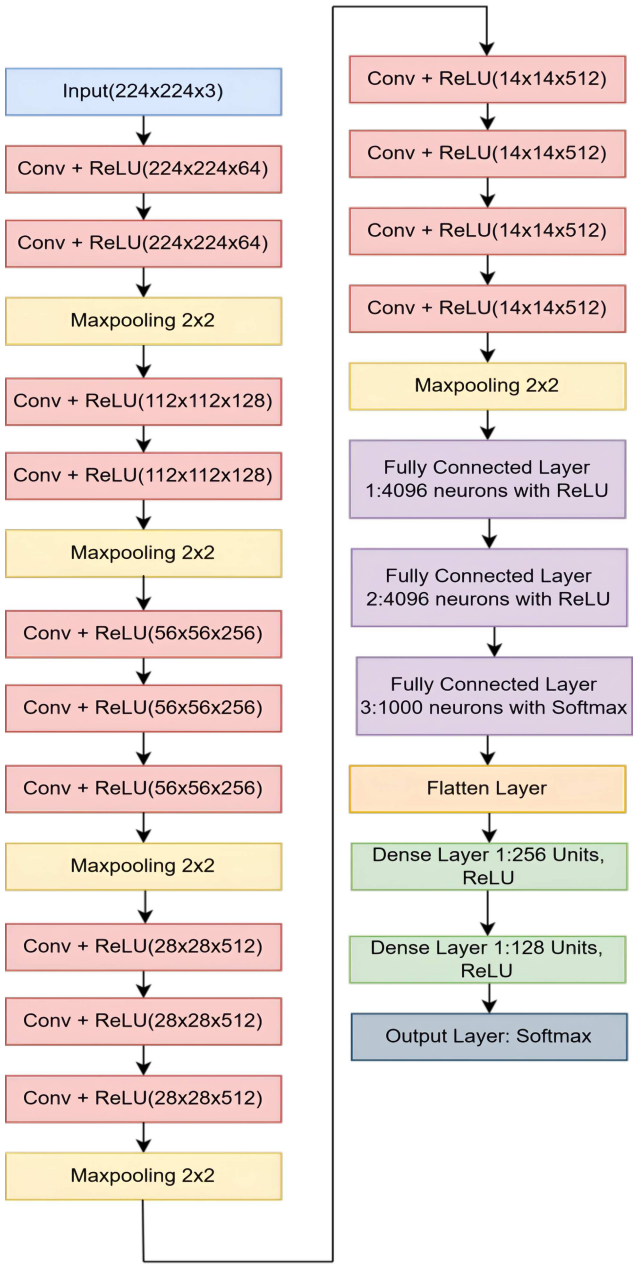

Figure 5
Activation maps from convolutional layers

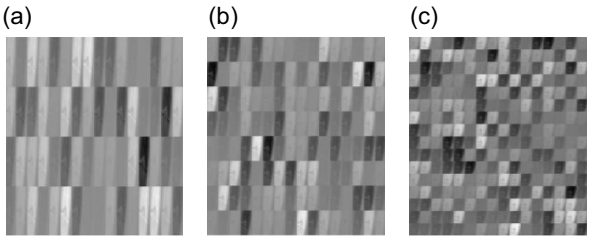

C1 Layer – 64 Activations **C2 Layer – 128 Activations** **C3 Layer – 256 Activations**

3.3. Transfer learning approach: VGG16 based

To enhance classification accuracy, a fine-tuned VGG16 model was employed as the second approach, as illustrated in Figure 6. VGG16 is a widely adopted CNN architecture, known for its robustness and effectiveness in image classification and feature extraction tasks. It consists of 16 weight layers, including 13 convolutional layers followed by 3 fully connected layers. The architecture is characterized by its uniform use of small 3 × 3 convolutional filters with a stride of 1, enabling the extraction of fine-grained image features while maintaining computational efficiency. Max pooling layers with a 2 × 2 window follow select convolutional blocks to downsample the spatial dimensions of the feature maps, thereby retaining essential features and reducing computational complexity. In the transfer learning setup, the pretrained VGG16 layers serve as a feature extractor, and the final fully connected layers are replaced with a new classifier head consisting of dense layers with ReLU activation and a softmax output layer, as shown in the final blocks of the architecture diagram. This approach leverages the learned representations from large-scale datasets (e.g., ImageNet) and fine-tunes the network on the target dataset, significantly reducing training time while improving accuracy and generalization.

3.4. Hybrid ensemble approach

In the proposed hybrid ensemble framework, the final KOA grade prediction is obtained by combining the outputs of two independent DL models: a custom CNN and a fine-tuned VGG16 transfer learning model. Each model processes the same preprocessed knee X-ray image and produces a probability distribution over the five KL grades (0–4) using a softmax layer, and its architecture is depicted in Figure 7.

Let $P_{CNN} = \left[P_0^{CNN}, P_1^{CNN}, P_2^{CNN}, P_3^{CNN}, P_4^{CNN}\right]$ denote the softmax probability vector obtained from the custom CNN, and $P_{VGG} = \left[P_0^{VGG}, P_1^{VGG}, P_2^{VGG}, P_3^{VGG}, P_4^{VGG}\right]$ represent the probability vector from the fine-tuned VGG16 model.

The ensemble probability for each KL grade k is computed using a weighted averaging strategy as:

$$P_{ensemble}(k) = w_{CNN}.P_k^{CNN} + w_{VGG}.P_k^{VGG} \quad (3)$$

Figure 6
Transfer learning approach

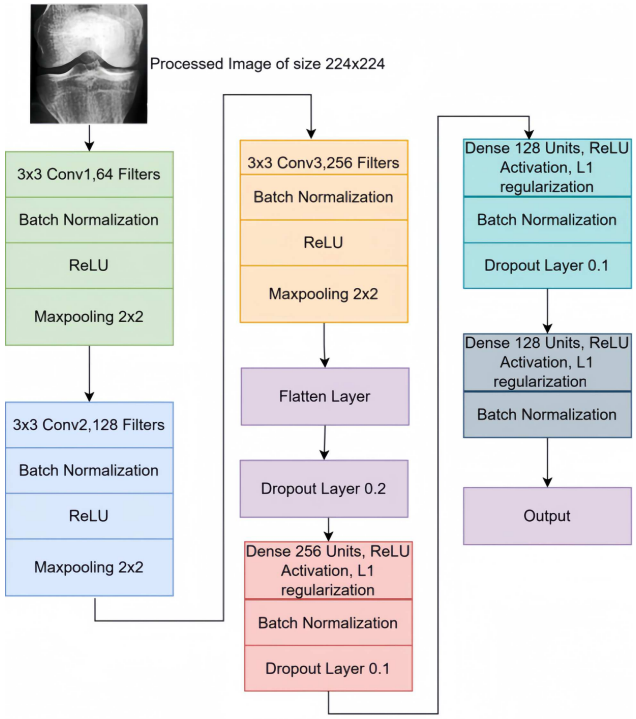

Figure 7
Proposed hybrid ensemble framework

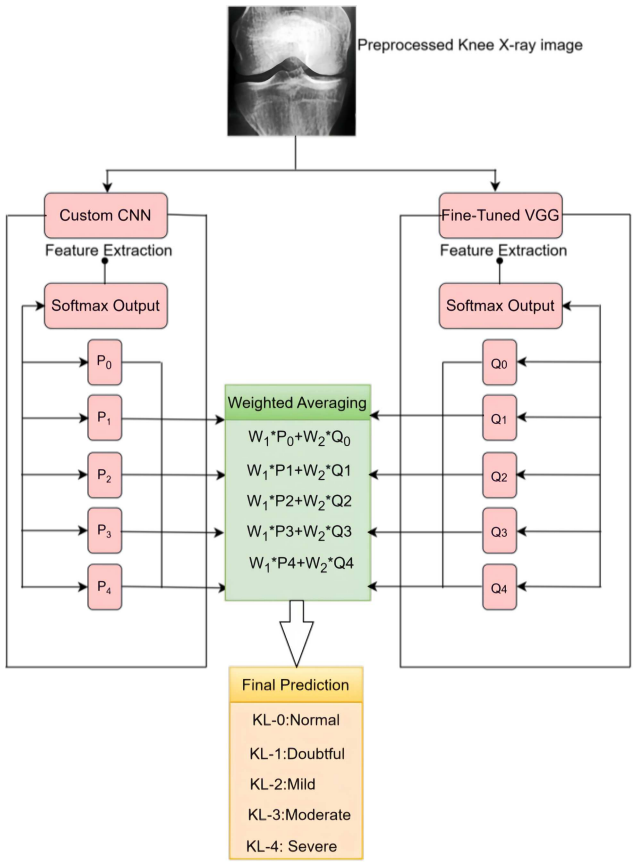

Subject to:

$$w_{CNN} + w_{VGG} = 1$$

At the initial stage, equal weights are assigned:

$W_{CNN} = 0.5$ and $W_{VGG} = 0.5$

This ensured an unbiased fusion of both models. Then, the weights were optimized using the validation set to maximize classification accuracy.

$$\left(w^*_{CNN}, w^*_{VGG}\right) = argmax\ Accuracy(P_{ensemble}) \tag{4}$$

The predicted KL grade is obtained by:

$$\hat{k} = arg^{max}_{k} P_{ensemble}\,(k)$$

This probability-level fusion allows the ensemble to exploit the complementary strengths of the two models—local texture learning from the custom CNN and deep hierarchical feature representation from VGG16—resulting in improved robustness and more reliable KOA severity classification, particularly for early disease stages.

3.5. Results and discussion

Data augmentation was employed to improve dataset diversity and enhance generalization. Images were randomly rotated up to 40°, shifted horizontally and vertically by 20% of the image dimensions, and subjected to shearing and zooming within a factor of 0.2. Horizontal flipping was also performed to introduce mirrored variations.

All images were resized to 224 × 224 pixels to meet model input requirements. The accuracy trends before and after augmentation for the custom CNN (CCNN), fine-tuned VGG16 (FVGG), and ensemble approach (EA) are summarized in Table 2. Precision, recall, and F1-score at 250 epochs are reported in Table 3. The results reveal a clear performance gap between the shallow CCNN and the VGG-based transfer learning model. For the CCNN, data augmentation led to a reduction in accuracy from 73.09% to 58.8% at 250 epochs, indicating limited capacity to learn the increased variability introduced by augmentation.

In contrast, the FVGG model demonstrated substantial improvement, with accuracy increasing from 90.0% to 96.8% after augmentation. This highlights the robustness of pretrained deep architectures in leveraging augmented data for improved generalization. The ensemble approach further improved performance by combining CCNN and FVGG predictions through softmax probability averaging, achieving a peak accuracy of 98%.

KL grade-wise performance of the proposed model is presented in Table 4. High sensitivity and specificity across grades indicate reliable detection of disease severity, particularly for early and moderate osteoarthritis stages. Comparative analysis with existing state-of-the-art methods (Table 5) confirms the superiority of the proposed transfer learning and ensemble approaches. Overall, these results demonstrate that the effectiveness of data augmentation is model-dependent—significantly benefiting deep pretrained networks such as VGG16, while offering limited or negative gains for shallow custom CNNs due to constrained feature-learning capacity.

3.6. Webpage design

The system designed for predicting KOA severity—categorized as Normal, Doubtful, Mild, Moderate, and

Table 2
Accuracy for the custom learning approach

Before data augmentation				After data augmentation			
Epochs	Accuracy (CCNN)(%)	Accuracy (FVGG)(%)	Accuracy (EA)(%)	Epochs	Accuracy (CCNN)(%)	Accuracy (FVGG)(%)	Accuracy (EA)(%)
50	72	85	85.7	50	58	95	95
100	72.2	87.5	86.5	100	58.7	95.5	96.5
150	73.4	89	87	150	59	95.8	96.6
200	72.8	89.5	88.6	200	59.3	96	97.8
225	75.3	89.5	90.9	225	60	96.6	97.8
250	73.09	90	90	250	58.8	96.8	98

Table 3
Overall accuracy

Model	Data augmentation	Epoch	Accuracy (%)	Precision (%)	Recall (%)	F1-score (%)
CCNN	No	250	73.09	74.5	75.0	74.7
CCNN	Yes	250	58.8	58.0	60.5	59.2
FVGG	No	250	90.0	89.0	90.5	89.7
FVGG	Yes	250	96.8	96.5	97.0	96.7
EA	No	250	91.5	91	92	91.5
EA	Yes	250	98	97.8	98.5	98.1

Table 4
KL grade-wise performance

KL grade	Sensitivity (%)	Specificity (%)	F1-score (%)
KL-0 (Normal)	98.5	95.6	97.5
KL-1 (Doubtful)	72.3	89.1	79.6
KL-2 (Mild)	75.5	82.2	77.1
KL-3 (Moderate)	79.7	85.9	76.6
KL-4 (Severe)	73.5	89.2	77.6

Table 5
Comparative analysis

Model	Accuracy (%)
ResNet-50 [31]	63.4
LSTM [32]	71.97
SVM [33]	67.71
GLCM + LBP [34]	69.7
12 Layer CNN [35]	92.3
Proposed custom approach	58.8
Proposed transfer learning approach	96.8
Ensemble approach	98

Figure 8
User interface of the knee osteoarthritis prediction web application

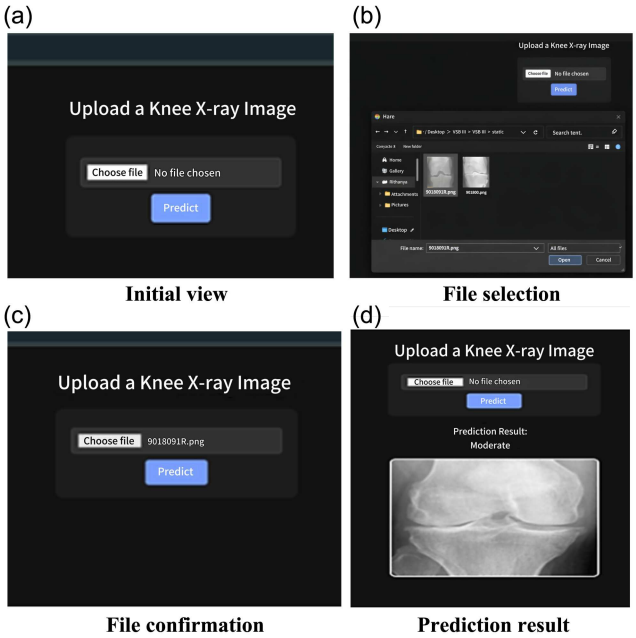

Severe—was implemented using Python in the IDLE environment. The deployment was facilitated using the Flask web framework, which enables seamless integration of ML models into a web-based application. In this setup, X-ray images are uploaded via the web interface, and the model processes them to generate the corresponding severity prediction. The application can be tested with a variety of X-ray inputs to evaluate its performance. Figure 8 illustrates the user interface of the developed web application, showcasing the step-by-step workflow, from launching the webpage to obtaining the prediction result.

4. Conclusion

OA of the knee is a disabling and frequent condition that significantly affects patients' quality of life and leads to a tremendous burden on healthcare systems. The use of ML in KOA research has been of immense utility in enhancing early diagnosis, disease progression prediction, and personalization of treatment. ML algorithms, particularly DL models, have shown that they can interpret medical images, detect risk factors, and maximize patient care. However, certain problems remain, including data limitations, model interpretability, and clinical adoption. Resolution of these issues is required to ensure that ML-based solutions become reliable and widely used in real healthcare environments. Despite the existing challenges, ML keeps improving and offers better prospects in KOA management. The future directions should involve improving data quality, developing explainable models, and improving clinical relevance. Improving these areas will enable ML to play a stronger role in KOA diagnosis and treatment.

Ethical Statement

This study used case images obtained from a publicly available dataset and does not contain any studies with human or animal subjects performed by any of the authors.

Conflicts of Interest

The authors declare that they have no conflicts of interest to this work.

Data Availability Statement

This study utilized data from the OAI database, a public resource available at https://nda.nih.gov/oai/. The OAI is a multicenter, longitudinal study of KOA, funded by the National Institutes of Health.

Author Contribution Statement

G. Prema: Conceptualization, Methodology, Validation, Formal analysis, Investigation, Resources, Data curation, Writing – review & editing, Visualization, Supervision, Project administration. **P. Rithanya:** Software, Resources, Data curation, Writing – original draft, Writing – review & editing, Visualization. **A. Shiva Priya:** Software, Resources, Data curation, Writing – original draft, Writing – review & editing, Visualization.

References

[1] Wang, Y., Bi, Z., Xie, Y., Wu, T., Zeng, X., Chen, S., & Zhou, D. (2022). Learning from highly confident samples for automatic knee osteoarthritis severity assessment: Data from the osteoarthritis initiative. *IEEE Journal of Biomedical and Health Informatics*, *26*(3), 1239–1250. https://doi.org/10.1109/JBHI.2021.3102090

[2] Saini, D., Chand, T., Chouhan, D. K., & Prakash, M. (2021). A comparative analysis of automatic classification and grading methods for knee osteoarthritis focussing on X-ray images. *Biocybernetics and Biomedical Engineering*, *41*(2), 419–444. https://doi.org/10.1016/j.bbe.2021.03.002

[3] Tiulpin, A., & Saarakkala, S. (2020). Automatic grading of individual knee osteoarthritis features in plain radiographs using deep convolutional neural networks. *Diagnostics*, *10*(11), 932. https://doi.org/10.3390/diagnostics10110932

[4] Chen, P., Gao, L., Shi, X., Allen, K., & Yang, L. (2019). Fully automatic knee osteoarthritis severity grading using deep neural networks with a novel ordinal loss. *Computerized Medical Imaging and Graphics*, *75*, 84–92. https://doi.org/10.1016/j.compmedimag.2019.06.002

[5] Nichols, C. J., Özmen, G. C., Richardson, K., Inan, O. T., & Ewart, D. (2023). Classifying pre-radiographic osteoarthritis of the knee using wearable acoustics sensing at the point of care. *IEEE Sensors Journal*, *23*(23), 29619–29629. https://doi.org/10.1109/JSEN.2023.3325153

[6] Badshah, Y., Shabbir, M., Hayat, H., Fatima, Z., Burki, A., Khan, S., & Rehman, S. U. (2021). Genetic markers of osteoarthritis: Early diagnosis in susceptible Pakistani population. *Journal of Orthopaedic Surgery and Research*, *16*(1), 124. https://doi.org/10.1186/s13018-021-02230-x

[7] Nasser, Y., Jennane, R., Chetouani, A., Lespessailles, E., & Hassouni, M. E. (2020). Discriminative regularized auto-encoder for early detection of knee osteoarthritis: Data from the osteoarthritis initiative. *IEEE Transactions on Medical Imaging*, *39*(9), 2976–2984. https://doi.org/10.1109/TMI.2020.2985861

[8] Brahim, A., Jennane, R., Riad, R., Janvier, T., Khedher, L., Toumi, H., & Lespessailles, E. (2019). A decision support tool for early detection of knee OsteoArthritis using X-ray imaging

and machine learning: Data from the OsteoArthritis Initiative. *Computerized Medical Imaging and Graphics*, *73*, 11–18. https://doi.org/10.1016/j.compmedimag.2019.01.007

[9] Zhang, B., Tan, J., Cho, K., Chang, G., & Deniz, C. M. (2020). Attention-based CNN for KL grade classification: Data from the osteoarthritis initiative. In *2020 IEEE 17th International Symposium on Biomedical Imaging* (pp. 731–735). https://doi.org/10.1109/ISBI45749.2020.9098456

[10] Kim, D. H., Lee, K. J., Choi, D., Lee, J. I., Choi, H. G., & Lee, Y. S. (2020). Can additional patient information improve the diagnostic performance of deep learning for the interpretation of knee osteoarthritis severity. *Journal of Clinical Medicine*, *9*(10), 3341. https://doi.org/10.3390/jcm9103341

[11] Yong, C. W., Teo, K., Murphy, B. P., Hum, Y. C., Tee, Y. K., Xia, K., & Lai, K. W. (2022). Knee osteoarthritis severity classification with ordinal regression module. *Multimedia Tools and Applications*, *81*(29), 41497–41509. https://doi.org/10.1007/s11042-021-10557-0

[12] Antony, J., McGuinness, K., Moran, K., & O'Connor, N. E. (2017). Automatic detection of knee joints and quantification of knee osteoarthritis severity using convolutional neural networks. In *Machine Learning and Data Mining in Pattern Recognition: 13th International Conference*, 376–390. https://doi.org/10.1007/978-3-319-62416-7_27

[13] Muhammad, M. B., & Yeasin, M. (2020). Eigen-CAM: Class activation map using principal components. In *2020 International Joint Conference on Neural Networks*, 1–7. https://doi.org/10.1109/IJCNN48605.2020.9206626

[14] Routson, R. L., Bailey, M., Pumford, I., Czerniecki, J. M., & Aubin, P. M. (2016). A smart cane with vibrotactile biofeedback improves cane loading for people with knee osteoarthritis. In *2016 38th Annual International Conference of the IEEE Engineering in Medicine and Biology Society*, 3370–3373. https://doi.org/10.1109/EMBC.2016.7591450

[15] Hu, K., Wu, W., Li, W., Simic, M., Zomaya, A., & Wang, Z. (2022). Adversarial evolving neural network for longitudinal knee osteoarthritis prediction. *IEEE Transactions on Medical Imaging*, *41*(11), 3207–3217. https://doi.org/10.1109/TMI.2022.3181060

[16] Wu, J., Qian, Z., Xu, R., Liu, J., Ren, L., & Ren, L. (2021). Association between pain in knee osteoarthritis and mechanical properties of soft tissue around knee joint. *IEEE Access*, *9*, 14599–14607. https://doi.org/10.1109/ACCESS.2021.3050776

[17] Dodin, P., Pelletier, J.-P., Martel-Pelletier, J., & Abram, F. (2010). Automatic human knee cartilage segmentation from 3-D magnetic resonance images. *IEEE Transactions on Biomedical Engineering*, *57*(11), 2699–2711. https://doi.org/10.1109/TBME.2010.2058112

[18] Kubota, K., Hanawa, H., Yokoyama, M., Kita, S., Hirata, K., Fujino, T., . . . , & Kanemura, N. (2021). Usefulness of muscle synergy analysis in individuals with knee osteoarthritis during gait. *IEEE Transactions on Neural Systems and Rehabilitation Engineering*, *29*, 239–248. https://doi.org/10.1109/TNSRE.2020.3043831

[19] Chen, X., Chen, J., Liang, J., Li, Y., Courtney, C. A., & Yang, Y. (2019). Entropy-based surface electromyogram feature extraction for knee osteoarthritis classification. *IEEE Access*, *7*, 164144–164151. https://doi.org/10.1109/ACCESS.2019.2950665

[20] Eugster, M., Zoller, E. I., Krenn, P., Blache, S., Friederich, N. F., Müller-Gerbl, M., . . . , & Rauter, G. (2021). Quantitative evaluation of the thickness of the available manipulation volume inside the knee joint capsule for minimally invasive robotic unicondylar knee arthroplasty. *IEEE Transactions on Biomedical Engineering*, *68*(8), 2412–2422. https://doi.org/10.1109/TBME.2020.3041512

[21] He, Z., Liu, T., & Yi, J. (2019). A wearable sensing and training system: Towards gait rehabilitation for elderly patients with knee osteoarthritis. *IEEE Sensors Journal*, *19*(14), 5936–5945. https://doi.org/10.1109/JSEN.2019.2908417

[22] Karim, M. R., Jiao, J., Dohmen, T., Cochez, M., Beyan, O., Rebholz-Schuhmann, D., & Decker, S. (2021). DeepKneeExplainer: Explainable knee osteoarthritis diagnosis from radiographs and magnetic resonance imaging. *IEEE Access*, *9*, 39757–39780. https://doi.org/10.1109/ACCESS.2021.3062493

[23] Kwon, S. B., Han, H.-S., Lee, M. C., Kim, H. C., Ku, Y., & Ro, D. H. (2020). Machine learning-based automatic classification of knee osteoarthritis severity using gait data and radiographic images. *IEEE Access*, *8*, 120597–120603. https://doi.org/10.1109/ACCESS.2020.3006335

[24] Lee, Y., Toan, B., Ahn, C., & Shin, J. (2014). Cartilage-defect assessment by measuring thickness of knee MRI: Data from the osteoarthritis initiative. In *The 18th IEEE International Symposium on Consumer Electronics* (pp. 1–2). https://doi.org/10.1109/ISCE.2014.6884524

[25] Marzorati, D., Sarti, M., Mainardi, L., Manzotti, A., & Cerveri, P. (2020). Deep 3D convolutional networks to segment bones affected by severe osteoarthritis in CT scans for PSI-based knee surgical planning. *IEEE Access*, *8*, 196394–196407. https://doi.org/10.1109/ACCESS.2020.3034418

[26] Munoz-Organero, M., Littlewood, C., Parker, J., Powell, L., Grindell, C., & Mawson, S. (2017). Identification of walking strategies of people with osteoarthritis of the knee using insole pressure sensors. *IEEE Sensors Journal*, *17*(12), 3909–3920. https://doi.org/10.1109/JSEN.2017.2696303

[27] Shamir, L., Ling, S. M., Scott, W. W., Bos, A., Orlov, N., Macura, T. J., . . . , & Goldberg, I. G. (2009). Knee X-ray image analysis method for automated detection of osteoarthritis. *IEEE Transactions on Biomedical Engineering*, *56*(2), 407–415. https://doi.org/10.1109/TBME.2008.2006025

[28] Tamez-Peña, J. G., Farber, J., González, P. C., Schreyer, E., Schneider, E., & Totterman, S. (2012). Unsupervised segmentation and quantification of anatomical knee features: Data from the Osteoarthritis Initiative. *IEEE Transactions on Biomedical Engineering*, *59*(4), 1177–1186. https://doi.org/10.1109/TBME.2012.2186612

[29] Wang, C., Chan, P. P. K., Lam, B. M. F., Wang, S., Zhang, J. H., Chan, Z. Y. S., . . . , & Cheung, R. T. H. (2020). Real-time estimation of knee adduction moment for gait retraining in patients with knee osteoarthritis. *IEEE Transactions on Neural Systems and Rehabilitation Engineering*, *28*(4), 888–894. https://doi.org/10.1109/TNSRE.2020.2978537

[30] Abdullah, S. S., & Rajasekaran, M. P. (2022). Automatic detection and classification of knee osteoarthritis using deep learning approach. *La Radiologia Medica*, *127*(4), 398–406. https://doi.org/10.1007/s11547-022-01476-7

[31] Wahyuningrum, R. T., Anifah, L., Eddy Purnama, I. K., & Hery Purnomo, M. (2019). A new approach to classify knee osteoarthritis severity from radiographic images based on CNN-LSTM method. In *2019 IEEE 10th International Conference on Awareness Science and Technology*, 1–6. https://doi.org/10.1109/ICAwST.2019.8923284

[32] Bonakdari, H., Jamshidi, A., Pelletier, J.-P., Abram, F., Tardif, G., & Martel-Pelletier, J. (2021). A warning machine learning algorithm for early knee osteoarthritis structural progressor patient screening. *Therapeutic Advances in Musculoskeletal Disease*, *13*, 1759720X21993254. https://doi.org/10.1177/1759720X21993254

[33] Yang, T., Zhu, H., Gao, X., Zhang, Y., Hui, Y., & Wang, F. (2020). Grading of metacarpophalangeal rheumatoid arthritis on ultrasound images using machine learning algorithms. *IEEE Access*, *8*, 67137–67146. https://doi.org/10.1109/ACCESS.2020.2982027

[34] Rani, S., Memoria, M., Almogren, A., Bharany, S., Joshi, K., Altameem, A., . . . , & Hamam, H. (2024). Deep learning to combat knee osteoarthritis and severity assessment by using CNN-based classification. *BMC Musculoskeletal Disorders*, *25*(1), 817. https://doi.org/10.1186/s12891-024-07942-9

[35] Zakerian, H., Yadollahzadeh-Tabari, M., Shirgahi, H., & Motameni, H. (2026). A hybrid invasive weed optimization–Convolutional neural network and bidirectional generative adversarial network for white blood cell image segmentation and classification in leukemia analysis. *International Journal of Engineering*, *39*(6), 1496–1508. https://doi.org/10.5829/ije.2026.39.06c.16

How to Cite: Prema, G., Rithanya, P., & Shiva Priya, A. (2026). Dual-Model Approach for Knee Osteoarthritis Classification Using Custom CNN and Fine-Tuned VGG16 with Histogram Equalization. *Smart Wearable Technology*. https://doi.org/10.47852/bonviewSWT62027989